N-WASP inhibitor wiskostatin nonselectively perturbs membrane transport by decreasing cellular ATP levels

Christopher J. Guerriero and Ora A. Weisz

Am J Physiol Cell Physiol 292:1562-1566, 2007. First published Nov 8, 2006;
doi:10.1152/ajpcell.00426.2006

Am J Physiol Cell Physiol 292: C1562–C1566, 2007.
First published November 8, 2006; doi:10.1152/ajpcell.00426.2006.

CALL FOR PAPERS | *Protein and Vesicle Trafficking, Cytoskeleton*

N-WASP inhibitor wiskostatin nonselectively perturbs membrane transport by decreasing cellular ATP levels

Christopher J. Guerriero and Ora A. Weisz

Renal-Electrolyte Division, Department of Medicine, University of Pittsburgh, Pittsburgh, Pennsylvania

Submitted 10 August 2006; accepted in final form 1 November 2006

Guerriero CJ, Weisz OA. N-WASP inhibitor wiskostatin nonselectively perturbs membrane transport by decreasing cellular ATP levels. *Am J Physiol Cell Physiol* 292: C1562–C1566, 2007. First published November 8, 2006; doi:10.1152/ajpcell.00426.2006.—Wiskott-Aldrich syndrome protein (WASP) and WAVE stimulate actin-related protein (Arp)2/3-mediated actin polymerization, leading to diverse downstream effects, including the formation and remodeling of cell surface protrusions, modulation of cell migration, and intracytoplasmic propulsion of organelles and pathogens. Selective inhibitors of individual Arp2/3 activators would enable more exact dissection of WASP- and WAVE-dependent cellular pathways and are potential therapeutic targets for viral pathogenesis. Wiskostatin is a recently described chemical inhibitor that selectively inhibits neuronal WASP (N-WASP)-mediated actin polymerization in vitro. A growing number of recent studies have utilized this drug in vivo to uncover novel cellular functions for N-WASP; however, the selectivity of wiskostatin in intact cells has not been carefully explored. In our studies with this drug, we observed rapid and dose-dependent inhibition of N-WASP-dependent membrane trafficking steps. Additionally, however, we found that addition of wiskostatin inhibited numerous other cellular functions that are not believed to be N-WASP dependent. Further studies revealed that wiskostatin treatment caused a rapid, profound, and irreversible decrease in cellular ATP levels, consistent with its global effects on cell function. Our data caution against the use of this drug as a selective perturbant of N-WASP-dependent actin dynamics in vivo.

phosphatidylinositol 4,5-bisphosphate; cytoskeleton; membrane traffic; Arp2/3; actin comets

THE DYNAMIC POLYMERIZATION of actin into straight or branched filaments regulates myriad and diverse cellular processes including ion transport, membrane trafficking, and cell migration (11, 20, 23). An important modulator of actin polymerization is the actin-related protein (Arp)2/3 complex, which nucleates the polymerization of actin on existing filaments to create a branched network. Members of the Wiskott-Aldrich syndrome protein (WASP) and SCAR/WAVE families of proteins activate Arp2/3-mediated actin polymerization, leading to distinct downstream effects. For example, Rac-mediated association of WAVE proteins with Arp2/3 regulates the formation of lamellopodia, whereas Cdc42- and phosphatidylinositol 4,5-bisphosphate (PIP_2)-stimulated binding of the ubiquitously expressed WASP family member neuronal WASP (N-WASP) to Arp2/3 has been implicated in the intracytoplasmic propulsion via actin comets of transport vesicles, organelles, and invading pathogens (8, 9, 25).

N-WASP contains multiple domains that contribute to its function, including a WASP homology (WH)1 domain, a GTPase binding domain (GBD), a proline-rich region, and a WA domain that binds to both actin and Arp2/3. The protein normally exists in an autoinhibited state that is maintained by *cis* interactions between the GBD and the conserved COOH-terminal WA domain. Interaction with GTP-bound Cdc42 and PIP_2 relieves the autoinhibition and promotes N-WASP-mediated activation of Arp2/3. Activation of Arp2/3 by WASP and WAVE proteins can be blocked in vivo by expression of the highly homologous WA domains of these proteins, which function as dominant-negative inhibitors (14). However, compounds that selectively inhibit individual members of these families would enable more precise identification of the roles of these proteins in Arp2/3-dependent cellular processes. Moreover, selective inhibition of N-WASP activation has potential therapeutic application in preventing the spread of infectious agents that utilize N-WASP-mediated pathways for transmission, including *Listeria monocytogenes*, *Shigella flexneri*, and vaccinia virus (3). To this end, wiskostatin, a chemical inhibitor of N-WASP, was recently identified in a high-throughput screen for inhibitors of PIP_2-mediated actin polymerization (19). In vitro studies demonstrated that wiskostatin binds to the GBD of N-WASP and thereby stabilizes the autoinhibited conformation of the protein (18). However, the selectivity of this drug has not been carefully tested in vivo.

A rapidly growing number of publications have reported the use of wiskostatin to assess the role of N-WASP in various cellular processes (5, 10, 12, 21, 26). In some cases, the effects of wiskostatin on these pathways were interpreted as evidence for known or novel roles for N-WASP in cellular pathways. For example, addition of 50 μM wiskostatin to intestinal epithelial cells was found to inhibit the formation of nascent adherens junctions (10). A more recent report found that addition of 10 μM wiskostatin to B16-F1 cells rapidly dispersed mTuba-containing puncta and inhibited membrane ruffling (12). Another report used 50 μM wiskostatin to show that N-WASP-mediated vesicle motility is a downstream event in nonclassic apoptosis triggered by the adenoviral protein E4orf4 (21). Finally, Haller et al. (5) used 40 μM wiskostatin to demonstrate that N-WASP activation is important for the maturation of immunologic synapses on T-lymphocyte stimulation.

During our own studies on the role of N-WASP in polarized biosynthetic traffic, we tested the effect of wiskostatin on a

Address for reprint requests and other correspondence: O. A. Weisz, Renal-Electrolyte Div., Univ. of Pittsburgh, 3550 Terrace St., Pittsburgh, PA 15261 (e-mail: weisz@pitt.edu).

The costs of publication of this article were defrayed in part by the payment of page charges. The article must therefore be hereby marked "*advertisement*" in accordance with 18 U.S.C. Section 1734 solely to indicate this fact.

transport step known to be disrupted by expression of dominant-negative inhibitors of N-WASP-mediated Arp2/3 activation. As predicted, treatment with wiskostatin significantly slowed delivery of apical proteins to the plasma membrane. However, in subsequent control experiments, we observed rapid and profound dose-dependent effects of this drug on many other cellular functions, including those that are not expected to be N-WASP dependent, such as protein synthesis and processing. The global effects of wiskostatin suggested that this drug may interfere with cellular energy stores. Indeed, treatment with wiskostatin at concentrations above 10 μM caused a precipitous and dose-dependent drop in cellular ATP levels that did not recover after washout. Our results suggest that wiskostatin does not function as a selective inhibitor of N-WASP dependent functions in intact cells but instead causes a global change in the energy status of cells that inhibits normal transport processes.

MATERIALS AND METHODS

Replication-defective recombinant adenoviruses. The generation of replication-defective recombinant adenoviruses encoding tetracycline-repressible influenza hemagglutinin (HA), murine phosphatidylinositol 4-phosphate 5-kinase-α (PI5K), and a control virus (where the coding sequence of a viral protein has been inserted in the reverse orientation) was described previously (4, 6).

Cell lines and adenoviral infection. Madin-Darby canine kidney (MDCK) type II cells stably expressing the tetracycline transactivator and the rabbit polymeric immunoglobulin receptor (pIgR) were cultured in modified Eagle's medium (Sigma) supplemented with 10% fetal bovine serum. For measurements of kinetics of surface delivery and transcytosis, cells were seeded at superconfluence in 12-mm Transwells (0.4-μm pore; Costar, Cambridge, MA) for 2–4 days before infection with recombinant adenoviruses at the following multiplicity of infection (control, PI5K, or WA: 250; HA: 50) as described in Ref. 6. For IgA transcytosis experiments, pIgR expression was enhanced by incubation with 2 mM butyrate for ≥16 h. Experiments were performed the following day.

Cell surface delivery assay. Filter-grown adenovirus-infected MDCK cells were starved for 30 min and radiolabeled for 15 min with 1 mCi/ml Trans-^{35}S-label (MP Biomedicals, Irvine, CA). To measure *trans*-Golgi network (TGN)-to-surface delivery of influenza HA, radiolabeled cells were chased 2 h at 19°C to stage newly synthesized membrane proteins in the TGN. The cells were then warmed rapidly to 37°C as indicated. Apical delivery of HA was measured by surface trypsinization as described in Ref. 7. Wiskostatin (Calbiochem; 11.7 mM stock in DMSO) or vehicle alone was added at the indicated times.

IgA transcytosis. MDCK cells stably expressing the rabbit pIgR were incubated with 5 μl of ^{125}I-labeled IgA for 10 min. Cells were washed extensively on ice before warming to 37°C for the indicated time periods. Wiskostatin was added at the indicated times and concentrations. Transcytosis was quantitated as described in Ref. 6.

Determination of cellular ATP levels. MDCK cells were plated at 50,000 cells/well in 12-well dishes (Costar). The following day the cells were treated for 0–1 h with either vehicle alone or wiskostatin (or sodium azide as a positive control) at the indicated concentrations and then solubilized by the method described in Ref. 27. Briefly, cells were washed twice with PBS followed by the addition of 1 ml of boiling distilled H_2O to each well, the cells were removed by pipetting, and the samples were centrifuged at 4°C for 5 min at 13,000 rpm to pellet debris. To assess the reversibility of drug treatment, cells were rinsed three times and incubated in fresh drug-free medium for 30 min before harvesting. To determine cellular ATP levels after treatment, 20 μl of each lysate was mixed with 100 μl of rLuciferase/Luciferin (Promega) and relative luminescence units were measured with a luminometer (Turner Designs TD-20.20). The ATP concentration in each sample was calculated by comparing the experimental values to a standard curve constructed with known concentrations of ATP and plotted as the percentage of control values obtained for mock-treated samples. Raw data were log transformed and analyzed by paired *t*-test. A P value of <0.05 was considered statistically different.

RESULTS

Wiskostatin inhibits Arp2/3-dependent apical biosynthetic traffic. We previously found that biosynthetic delivery of the marker protein HA from the TGN to the apical membrane of polarized MDCK cells is mediated by an N-WASP-Arp2/3-dependent mechanism (4). Adenovirus-mediated expression of a dominant-negative construct homologous to the WA domain of N-WASP inhibits apical delivery of HA, whereas activation of N-WASP on overexpression of PI5K stimulates HA delivery kinetics (4). On the basis of these data we hypothesized that wiskostatin would inhibit HA delivery to a level comparable to that of WA expression. HA-expressing MDCK cells (control or overexpressing PI5K) were radiolabeled for 15 min, incubated at 19°C to stage newly synthesized membrane proteins in the TGN, and then warmed to 37°C, and HA surface delivery was monitored after 1 h with a surface trypsinization assay as described in Ref. 7. As observed previously, HA delivery was stimulated relative to control in cells overexpressing PI5K and inhibited by expression of WA (Fig. 1*A*). Inclusion of 50 μM wiskostatin during the 37°C chase period caused a profound inhibition of HA delivery in both control and PI5K-overexpressing cells. In contrast, the effect of WA domain expression on HA delivery was largely rescued by PI5K coexpression.

We next examined the dose dependence of wiskostatin's effect on HA delivery. HA-expressing MDCK cells were radiolabeled, HA was staged in the TGN at 19°C for 2 h, and 10–50 μM wiskostatin or vehicle alone was added to the cells before warming to 37°C and quantitation of surface delivery kinetics. Additionally, some samples were treated with 50 μM wiskostatin during the 2-h stage and then washed extensively before warming to 37°C to assess the reversibility of wiskostatin's effect (Fig. 1*B*). HA surface delivery was unaffected by acute addition of 10 μM wiskostatin, but treatment with higher concentrations (25 or 50 μM) resulted in a virtual blockade in apical delivery. Moreover, the effect of wiskostatin treatment was irreversible over this period, because washout of the drug before warming failed to restore normal delivery kinetics.

Wiskostatin inhibits N-WASP-independent steps in transport. As a control to ensure the selectivity of wiskostatin for N-WASP-dependent cellular processes, we examined the effect of this drug on early steps in biosynthetic transport that are thought to be N-WASP independent (2, 4). MDCK cells expressing HA were starved in methionine-free medium, radiolabeled for 15 min, incubated for 2 h at 19°C to accumulate mature (sialylated) HA in the TGN, and then either solubilized or warmed to 37°C for 1 h, and surface delivery was assessed (Fig. 2). Wiskostatin (50, 25, or 10 μM) was added at various stages during this pulse-chase protocol. Addition of wiskostatin for 2 h at 19°C after the radiolabeling period decreased the accumulation of sialylated HA compared with a mock-treated sample in a dose-dependent manner (Fig. 2, *lanes C* and *A*, respectively), consistent with inhibition of either intra-Golgi

transport or the cellular glycosylation processing machinery. On subsequent warming to 37°C in the continued presence of wiskostatin, only 1.8% (50 μM), 2.7% (25 μM), or 20% (10 μM) of the total HA reached the cell surface in wiskostatin-treated cells (Fig. 2, *lane D*). In contrast, 53% of the total HA in mock-treated samples reached the surface during this period, as assessed by the susceptibility of HA to cleavage into HA1 and HA2 fragments on surface trypsinization (Fig. 2, *lane E*). Moreover, when wiskostatin was added to cells during the 30-min starvation period and in subsequent steps, we observed a loss in the synthesis of radiolabeled HA, particularly at the higher wiskostatin concentrations (Fig. 2, *lane B*). In cells treated with 50 μM wiskostatin during the starve and pulse, HA recovery was decreased by 92% compared with control, whereas 25 μM and 10 μM wiskostatin decreased recovery by 28% and 7.3%, respectively. Thus wiskostatin appears to inhibit uptake of radioactive methionine and/or disrupt protein synthesis.

Our results described above suggested that wiskostatin inhibits multiple steps along the biosynthetic pathway. To examine its role in postendocytic transport, we measured the effect of wiskostatin on basolateral-to-apical transcytosis of IgA in MDCK cells stably expressing the rabbit pIgR. In this multistep pathway, IgA binds to pIgR at the basolateral cell surface and is transported across the cell, where pIgR is cleaved to release a soluble IgA-pIgR complex into the apical medium. Transcytosis of IgA in these cells has previously been demonstrated to be actin dependent (15). MDCK cells were incubated for 10 min at 37°C with basolaterally added ^{125}I-IgA, washed extensively on ice, and then warmed to 37°C in the presence or absence of the indicated concentrations of wiskostatin. Transcytosis was quantitated as the release of ^{125}I-IgA into the apical medium as described in Ref. 6. Transcytosis was rapid and efficient, approaching 80% of the internalized ^{125}I-IgA within 1 h of warm-up (Fig. 3). In contrast, transcytosis was rapidly inhibited in a dose-dependent manner when wiskostatin was added to the cells at the start of the 37°C warm-up period. Inhibition of ^{125}I-IgA transcytosis by wiskostatin could reflect

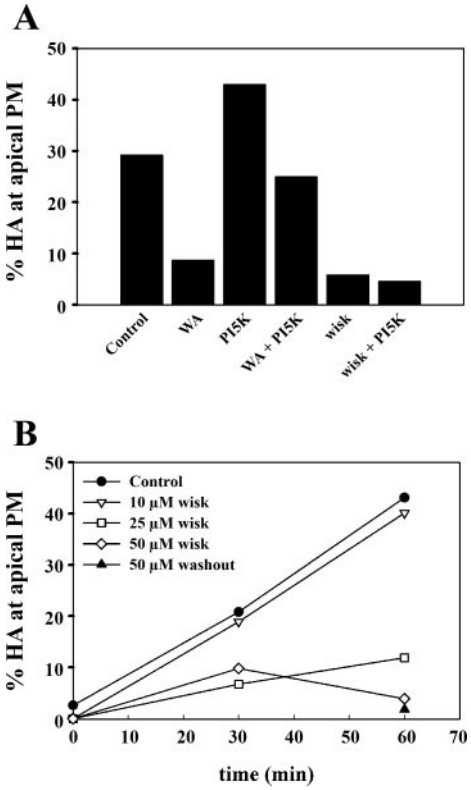

Fig. 1. Wiskostatin inhibits neuronal Wiskott-Aldrich syndrome protein (N-WASP)-dependent steps in membrane transport. *A*: polarized Madin-Darby canine kidney (MDCK) cells were infected with replication-defective recombinant adenoviruses encoding influenza hemagglutinin (HA) and phosphatidylinositol 4-phosphate 5-kinase (PI5K) and/or a construct encoding a dominant-negative inhibitor of N-WASP function (WA) as indicated. The following day, cells were radiolabeled for 15 min and chased for 2 h at 19°C to accumulate newly synthesized proteins in the *trans*-Golgi network. Apical delivery of HA was quantitated after warming to 37°C for 1 h in the presence or absence of 50 μM wiskostatin (wisk). *B*: cells were prepared as in *A* and were treated with wiskostatin at the indicated concentrations or with 50 μM wiskostatin during the 2-h chase followed by washout before warming to 37°C. The results of a single experiment in each case are shown. PM, plasma membrane.

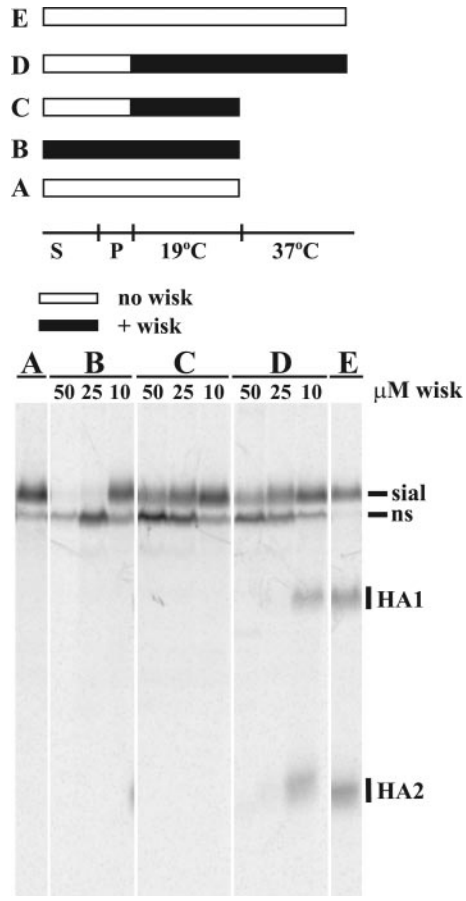

Fig. 2. Wiskostatin inhibits N-WASP-independent steps in protein processing. HA-expressing MDCK cells were starved (S) for 30 min, radiolabeled (P) for 15 min, incubated for 2 h at 19°C ,and then either solubilized immediately (samples in *lanes A*, *B*, and *C*) or incubated for 1 h at 37°C and trypsinized to quantitate surface delivery of HA before solubilization. HA was visualized after immunoprecipitation and SDS-PAGE. Samples in *lanes A* and *E* were mock-treated, whereas wiskostatin was added to the remaining samples beginning at the starve (*lane B*) or at the start of the 19°C incubation (*lanes C* and *D*). The migration of immature (ns) and sialylated (sial) forms of HA as well as the cleavage products generated on surface trypsinization (HA1 and HA2) are indicated. Surface delivery of HA in the samples in *lanes D* and *E* was 1.8% (50 μM), 2.7% (25 μM), 20% (10 μM), and 53% (control, *lane E*) of the total HA. Similar results were obtained in 2 experiments.

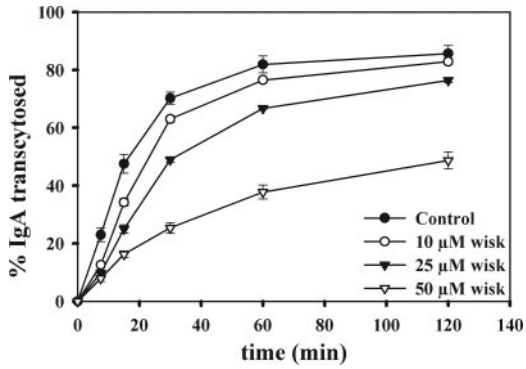

Fig. 3. Wiskostatin inhibits actin-dependent postendocytic membrane trafficking steps. Polarized MDCK cells were incubated with basolaterally added ^{125}I-labeled IgA for 10 min at 37°C and then washed extensively on ice. Apical release of ^{125}I-IgA was quantitated on warming to 37°C in the presence or absence of the indicated concentrations of wiskostatin added after IgA internalization. Means ± SD of triplicate samples are plotted.

a block in membrane traffic or, alternatively, inhibition of the proteolysis step required for the apical release of secretory component. However, when 50 μM wiskostatin was added to cells before the incubation with ^{125}I-IgA, internalization of the radioligand was completely inhibited (data not shown).

Wiskostatin decreases cellular ATP levels. It was shown previously that depletion of cellular ATP by energy poisons such as sodium azide dramatically inhibits protein processing and secretion (17). The rapid and profound effects of wiskostatin on multiple steps in protein synthesis, endocytosis, and membrane traffic suggested that this drug may similarly perturb cellular ATP levels. To examine this possibility, MDCK cells plated in 12-well dishes were treated with wiskostatin at 10, 25, or 50 μM or vehicle for 0–1 h at 37°C. ATP was extracted and quantified with a luminometry-based assay (Fig. 4). Addition of 25 μM and 50 μM wiskostatin, respectively, resulted in the rapid and nearly complete loss of cellular ATP, decreasing the levels to 57% and 30% of control within 15 min and to 18% and 9.4% of control within 1 h. Treatment with 2% sodium azide resulted in a comparable drop in ATP levels, to 4.6% of control after 1 h of treatment (not shown). Wiskostatin added at a lower concentration (10 μM) had a less dramatic effect on cellular ATP in MDCK cells (84% and 81% of control at 15 min and 1 h, respectively). Washout of the drug for 30 min after a 1-h treatment with any concentration of wiskostatin did not restore normal ATP levels, suggesting that the effects of the drug on cellular energy status are irreversible over this time period.

DISCUSSION

The studies described above suggest that wiskostatin has global and likely nonspecific effects on membrane traffic and other pathways. Treatment of polarized MDCK cells with this drug inhibited protein synthesis and maturation and disrupted both biosynthetic and postendocytic traffic. The effects of wiskostatin on these transport steps were dose dependent and irreversible and roughly paralleled in magnitude the effects of the drug on cellular ATP levels. Notably, however, gross cellular morphology and actin structure were not visibly altered after a 1-h incubation with 50 μM wiskostatin, indicating that cell death was not occurring during this period (data not shown).

We can only speculate as to the mechanism by which wiskostatin perturbs cellular ATP levels. Metabolic energy poisons fall into one of four classes, the first two of which are most common: *1*) inhibitors of electron transport, *2*) uncouplers/ionophores, *3*) inhibitors of ATP synthase, and *4*) inhibitors of transport systems (22). Members of the first group include rotenone, cyanide, and sodium azide, which block electron transport by interacting irreversibly or competitively with components of the electron transport chain (1, 16). The second group includes 2,4-dinitrophenol (DNP) and carbonyl cyanide *p*-trifluoromethoxyphenylhydrazone (FCCP), which disrupt the proton gradient by acting as proton ionophores (13, 24). The aromatic structure of wiskostatin suggests the possibility that, like DNP, it may also disrupt membrane integrity; however, elucidating the mechanism by which this drug interferes with cellular ATP homeostasis requires further study.

The effect of wiskostatin on most cellular transport steps and on ATP levels demonstrated a steep dose-dependent response at concentrations between 10 and 25 μM. Treatment with 10 μM wiskostatin decreased ATP levels by only ~20% after a 1-h treatment and had comparable effects on protein synthesis and maturation when added acutely to cells (Fig. 2, *lanes B* and *C*). In contrast, treatment with 25 μM wiskostatin decreased ATP levels by 80% over this time period. Interestingly, 10 μM wiskostatin did not affect the efficiency of surface delivery when added acutely after cargo had been prestaged in the TGN (Fig. 1*B*); however, surface delivery (but not HA maturation) was severely compromised (by 80%) when the drug was added at the start of the 2-h TGN staging period at 19°C (Fig. 2, *lane D*). A possible explanation is that post-Golgi transport may be insensitive to acute ATP depletion compared with other steps; however, longer incubations with this concentration of wiskostatin might sufficiently affect ATP levels to inhibit this step or otherwise disrupt other cellular functions required for efficient membrane traffic. Ironically, it is this very step in membrane transport, namely TGN-to-apical surface delivery of HA, that we previously found to be N-WASP dependent based on our

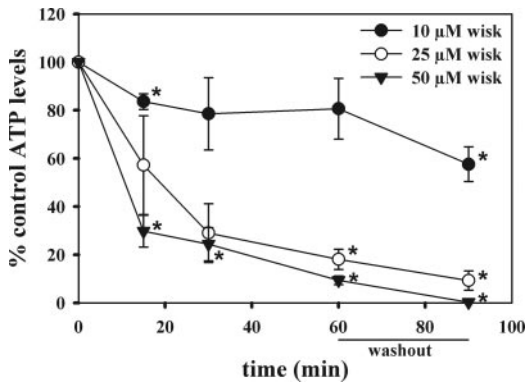

Fig. 4. Wiskostatin reduces cellular ATP levels. MDCK cells plated in 12-well dishes were treated with vehicle alone or with wiskostatin at 50, 25, or 10 μM for the indicated time periods. Some drug-treated samples were washed extensively after 1 h of treatment and incubated for an additional 30 min (washout) before assessment of cellular ATP levels as described in MATERIALS AND METHODS. The dose- and time-dependent effect of wiskostatin on ATP levels was normalized to control cells and plotted (means ± SE of 3 independent experiments). *$P < 0.05$ compared with control based on paired *t*-test of log-transformed raw data. Treatment with the known energy poison sodium azide (2%) decreased cellular ATP levels to 4.6% of control after 1 h of treatment (not shown).

studies using dominant-negative inhibitors of Arp2/3 activation (4). Previously published studies have utilized variable concentrations of wiskostatin, ranging from 10 to 50 μM (5, 10, 12, 21, 26). In all of these reports, rapid and profound effects on the particular cellular function being studied were noted and ascribed to selective inhibition of an N-WASP-dependent pathway. Given the global effects of wiskostatin on cellular transport processes and ATP levels, however, it is clear that this drug is inappropriate for in vivo studies aimed at selectively perturbing N-WASP function, or for potential therapeutic use as previously suggested (19). Moreover, novel roles ascribed to N-WASP in cellular pathways based solely on in vivo effects observed with wiskostatin merit careful reexamination.

ACKNOWLEDGMENTS

We thank Dr. Gerard Apodaca for thoughtful comments on the manuscript.

GRANTS

This work was supported by grants from the National Institute of Diabetes and Digestive and Kidney Diseases (NIDDK) (DK-064613) and the Commonwealth of Pennsylvania to O. A. Weisz. C. J. Guerriero was supported by NIDDK Grant T32-DK-61296 and a predoctoral award from the American Heart Association.

REFERENCES

1. **Ball EG, Cooper O.** The reaction of cytochrome oxidase with cyanide. *J Biol Chem* 198: 629–638, 1952.
2. **Duran JM, Valderrama F, Castel S, Magdalena J, Tomas M, Hosoya H, Renau-Piqueras J, Malhotra V, Egea G.** Myosin motors and not actin comets are mediators of the actin-based Golgi-to-endoplasmic reticulum protein transport. *Mol Biol Cell* 14: 445–459, 2003.
3. **Gouin E, Welch MD, Cossart P.** Actin-based motility of intracellular pathogens. *Curr Opin Microbiol* 8: 35–45, 2005.
4. **Guerriero CJ, Weixel KM, Bruns JR, Weisz OA.** Phosphatidylinositol 5-kinase stimulates apical biosynthetic delivery via an Arp2/3-dependent mechanism. *J Biol Chem* 281: 15376–15384, 2006.
5. **Haller C, Rauch S, Michel N, Hannemann S, Lehmann MJ, Keppler OT, Fackler OT.** The HIV-1 pathogenicity factor Nef interferes with maturation of stimulatory T-lymphocyte contacts by modulation of N-Wasp activity. *J Biol Chem* 281: 19618–19630, 2006.
6. **Henkel JR, Apodaca G, Altschuler Y, Hardy S, Weisz OA.** Selective perturbation of apical membrane traffic by expression of influenza virus M2, an acid-activated ion channel, in polarized Madin-Darby canine kidney cells. *Mol Biol Cell* 8: 2477–2490, 1998.
7. **Henkel JR, Gibson GA, Poland PA, Ellis MA, Hughey RP, Weisz OA.** Influenza M2 proton channel activity selectively inhibits TGN release of apical membrane and secreted proteins in polarized MDCK cells. *J Cell Biol* 148: 495–504, 2000.
8. **Higgs HN, Pollard TD.** Regulation of actin filament network formation through ARP2/3 complex: activation by a diverse array of proteins. *Annu Rev Biochem* 70: 649–676, 2001.
9. **Ibarra N, Pollitt A, Insall RH.** Regulation of actin assembly by SCAR/WAVE proteins. *Biochem Soc Trans* 33: 1243–1246, 2005.
10. **Ivanov AI, Hunt D, Utech M, Nusrat A, Parkos CA.** Differential roles for actin polymerization and a myosin II motor in assembly of the epithelial apical junctional complex. *Mol Biol Cell* 16: 2636–2650, 2005.
11. **Khurana S.** Role of actin cytoskeleton in regulation of ion transport: examples from epithelial cells. *J Membr Biol* 178: 73–87, 2000.
12. **Kovacs EM, Makar RS, Gertler FB.** Tuba stimulates intracellular N-WASP-dependent actin assembly. *J Cell Sci* 119: 2715–2726, 2006.
13. **Linnett PE, Beechey RB.** Inhibitors of the ATP synthetase system. *Methods Enzymol* 55: 472–518, 1979.
14. **Machesky LM, Insall RH.** Scar1 and the related Wiskott-Aldrich syndrome protein, WASP, regulate the actin cytoskeleton through the Arp2/3 complex. *Curr Biol* 8: 1347–1356, 1998.
15. **Maples CJ, Ruiz WG, Apodaca G.** Both microtubules and actin filaments are required for efficient postendocytic traffic of the polymeric immunoglobulin receptor in polarized Madin-Darby canine kidney cells. *J Biol Chem* 272: 6741–6751, 1996.
16. **Oberg KE.** The site of the action of rotenone in the respiratory chain. *Exp Cell Res* 24: 163–164, 1961.
17. **Persson R, Ahlstrom E, Fries E.** Differential arrest of secretory protein transport in cultured rat hepatocytes by azide treatment. *J Cell Biol* 107: 2503–2510, 1988.
18. **Peterson JR, Bickford LC, Morgan D, Kim AS, Ouerfelli O, Kirschner MW, Rosen MK.** Chemical inhibition of N-WASP by stabilization of a native autoinhibited conformation. *Nat Struct Mol Biol* 11: 747–755, 2004.
19. **Peterson JR, Lokey RS, Mitchison TJ, Kirschner MW.** A chemical inhibitor of N-WASP reveals a new mechanism for targeting protein interactions. *Proc Natl Acad Sci USA* 98: 10624–10629, 2001.
20. **Pollard TD, Borisy GG.** Cellular motility driven by assembly and disassembly of actin filaments. *Cell* 112: 453–465, 2003.
21. **Robert A, Smadja-Lamere N, Landry MC, Champagne C, Petrie R, Lamarche-Vane N, Hosoya H, Lavoie JN.** Adenovirus E4orf4 hijacks rho GTPase-dependent actin dynamics to kill cells: a role for endosome-associated actin assembly. *Mol Biol Cell* 17: 3329–3344, 2006.
22. **Scheffler IE.** *Mitochondria*. New York: Wiley, 1999.
23. **Stamnes M.** Regulating the actin cytoskeleton during vesicular transport. *Curr Opin Cell Biol* 14: 428–433, 2002.
24. **Stubbs M.** Inhibitors of the adenine nucleotide translocase. *Pharmacol Ther* 7: 329–350, 1979.
25. **Takenawa T, Miki H.** WASP and WAVE family proteins: key molecules for rapid rearrangement of cortical actin filaments and cell movement. *J Cell Sci* 114: 1801–1809, 2001.
26. **Ten Klooster JP, Evers EE, Janssen L, Machesky LM, Michiels F, Hordijk P, Collard JG.** Interaction between Tiam1 and the Arp2/3 complex links activation of Rac to actin polymerization. *Biochem J* 397: 39–45, 2006.
27. **Yang NC, Ho WM, Chen YH, Hu ML.** A convenient one-step extraction of cellular ATP using boiling water for the luciferin-luciferase assay of ATP. *Anal Biochem* 306: 323–327, 2002.